



**AIAA 93-0039**  
**Constrained Optimization of**  
**Three-Dimensional Hypersonic**  
**Vehicle Configurations**

**S. G. Sheffer and G.S. Dulikravich**  
**The Pennsylvania State University**  
**University Park, PA**

**31st Aerospace Sciences**  
**Meeting & Exhibit**  
**January 11-14, 1993 / Reno, NV**

# CONSTRAINED OPTIMIZATION OF THREE-DIMENSIONAL HYPERSONIC VEHICLE CONFIGURATIONS

Scott G. Sheffer<sup>1</sup> and George S. Dulikravich<sup>2</sup>  
 Department of Aerospace Engineering, 233 Hammond Building  
 The Pennsylvania State University, University Park, PA 16802, USA

## ABSTRACT

A new method has been developed for preliminary design optimization of arbitrary (non-axisymmetric) hypersonic configurations in terms of aerodynamic wave drag. This optimization was accomplished while fixing certain parts of the geometry and maintaining the initial volume and length of the vehicle. Because of the large number of flow analysis evaluations required by this optimization algorithm, a fast and accurate analysis code based on modified Newtonian flow theory was used. This shape optimization method utilized an independent point-motion algorithm for each surface point. The spatial locations of the points defining each cross section were varied and a numerical optimization algorithm based on a quasi-Newton gradient search concept was used to determine the new optimal configuration. Two different configurations were optimized: a cone and a hypersonic plane configuration. Each of these configurations had certain individual cross sections or surface points fixed during the optimization process. Numerical results indicate a significant decrease in aerodynamic wave drag for simple and complex configurations at a low computing cost. The procedure is capable of accepting more complex flow field analysis codes.

## NOMENCLATURE

$A$	= area of a panel on the body surface
$C_p$	= surface pressure coefficient
$C_{p0}$	= stagnation pressure coefficient
$F$	= aerodynamic force applied to a panel
$FAC$	= percentage change in design variable, used in finite difference approximation
$M_\infty$	= free stream Mach number
$\hat{n}$	= unit normal to the body surface

$p$	= static pressure at a point
$p_\infty$	= free stream static pressure
$u$	= velocity
$x$	= Cartesian coordinate along the axis
$y, z$	= Cartesian coordinates of a contour point at cross section $i$
$\gamma$	= specific heat ratio of the gas
$\Sigma$	= summation
$\theta_n$	= angle between free stream and normal to the surface of a vehicle

## Subscripts

$i$	= $i$ th cross section of the vehicle
$j$	= $j$ th point of a cross section contour
$\infty$	= free stream value

## INTRODUCTION

Although optimization of hypersonic bodies having axisymmetric and superelliptic (Lamé curve) cross sections has been accomplished in the past [1,2], the aerodynamic drag minimization of an arbitrary winged hypersonic vehicle has not been attempted [3] until recently [4]. The objective of this paper is to present a constrained shape optimization procedure for arbitrarily shaped hypersonic vehicles. While there are certainly some limitations of the methodologies used in this paper, it demonstrates that optimization of numerous variables can indeed be done and that this can be applied to complex configurations where sections or individual points of the configuration may be kept fixed.

In hypersonic flow ( $M_\infty > 5.0$ ), for preliminary design optimization purposes, the flow around an object may be modeled using an impact flow theory. In this theory, oncoming particles strike the surface of the object and impart the normal component of their momentum to that body. Classical Newtonian flow theory has been shown to approach reality when the free stream Mach number approaches infinity and the value of the ratio of specific heats approaches  $\gamma = 1$  [5]. Modified Newtonian theory has been shown to be quite satisfactory for predicting the aerodynamic forces and moments on a body [6]. It has the main advantage of being extremely simple, accurate [7] and fast when faced with the thousands of flow field

<sup>1</sup>Research Assistant. Student Member AIAA.

<sup>2</sup>Associate Professor. Associate Fellow AIAA.

Copyright © 1992 by George S. Dulikravich. Published by the American Institute of Aeronautics and Astronautics, Inc. with permission.

calculations needed in an optimization problem of this scope. Because of the use of modified Newtonian theory, it was implicitly assumed that the flow field was inviscid.

Modified Newtonian impact flow theory was used with a modified Newtonian constrained search optimization routine [8] that was based on the theoretical work of Pshenichny and Danilin [9] to obtain vehicle shapes which had significantly lower wave drag in hypersonic flow. In previous studies, cross section coordinates of the body were represented with curve-fitted Fourier series [4,10]. The coefficients of the Fourier series, one set representing the y coordinate and one set representing the z coordinate, with x as the axis coordinate of the vehicle, then became the design variables that were fed to the optimization routine. The optimization routine sequentially perturbed each of the coefficients by a small amount and determined the new shape that reduced wave drag while keeping the volume and length of the vehicle constant.

In this study, the y and z coordinates of the vehicle's cross sections were used as the design variables directly. The user determined which points of the cross section would be allowed to be altered and which would be constrained to remain fixed. The optimization routine perturbed separately each of the coordinates at each of the chosen cross section contour points. Then, it combined the changes into a new shape with lower wave drag while still honoring the global constraints of constant volume and constant length of the vehicle.

## NUMERICAL MODELS

The local surface pressure coefficient,  $C_{p,ij}$ , was calculated by the use of modified Newtonian impact flow theory [6], which states that

$$C_{p,ij} = C_{po} \cos^2 \theta_{n,ij} \quad (1)$$

where  $\theta_{n,ij}$  is the angle between the free stream and the normal to the surface at the point i,j. The stagnation pressure coefficient,  $C_{po}$ , is given by

$$C_{po} = \frac{2}{\gamma M_\infty^2} \left[ \left( \frac{\gamma + 1}{2\gamma M_\infty^2 - \gamma + 1} \right)^{\frac{1}{\gamma-1}} \left( \frac{\gamma+1}{2} M_\infty^2 \right)^{\frac{\gamma}{\gamma-1}} - 1 \right] \quad (2)$$

The pressure on a given segment of the body may then be calculated from the rearranged formula for  $C_{p,ij}$ , that is

$$P_{ij} = P_\infty + \frac{1}{2} C_{p,ij} \gamma P_\infty M_\infty^2 \quad (3)$$

The aerodynamic force on each surface panel is found from

$$\bar{F}_{ij} = - P_{ij} A_{ij} \hat{n}_{ij} \quad (4)$$

so that the resultant force on the entire body is obtained by summing all of the panel forces

$$\bar{F}_{total} = \sum_{ij} \bar{F}_{ij} \quad (5)$$

Aerodynamic wave drag was then the x-component of the resultant aerodynamic force.

After perturbing all of the y and z coordinates of the cross sections' points and analyzing these new perturbed shapes, the optimization algorithm combined the changes into a new shape that met the global constraints of constant volume and constant length, but which had a reduced aerodynamic wave drag.

## RESULTS

Based on modified Newtonian impact theory, a hypersonic analysis code was developed for arbitrary three-dimensional configurations. It was combined with a modified Newtonian search algorithm developed by Prof. A. Belegundu [8] that is based on the book by Pshenichny and Danilin [9]. Gradients of the cost function and constraints were determined with finite difference approximations. Convergence criteria was set as a change in drag of less than 0.1% between two successive optimization cycles. All computations were performed on Penn State's IBM 3090-600S.

Two test cases, a circular cone and a hypersonic plane, were run using the point motion algorithm. In these cases, individual points were constrained to remain constant throughout the optimization. FAC, the percentage change in each surface coordinate used in the finite difference approximation, was set at 5%. Both cases were run at an angle of attack of  $0^\circ$ , a specific heat ratio of  $\gamma = 1.4$  and a free stream Mach number of  $M_\infty = 10$ . Inviscid modified Newtonian theory was used as the flow field analysis routine. Notice that the values for  $\gamma$  and  $M_\infty$  appear in  $C_{po}$  which may be factored out of the pressure coefficient ratio thus affecting the numerical amount of inviscid drag, but not the qualitative amount of inviscid drag. The x-axis for each case was chosen to coincide with the long axis of the body. The y and z-axes were then mutually perpendicular to the x-axis.

A right circular cone was optimized keeping both the tip cross section and one cross section in the middle of the body constant. There were seven cross sections with 20 points per cross section. With two

cross sections being held constant, this yielded 100 points that could be perturbed resulting in 200 design variables (y and z coordinates of the surface points). The original and final optimized shapes are shown in Figures 1, 2 and 3. A 25.2% drag reduction was achieved after 39 optimization cycles. It may be seen that the constrained cross sections did remain fixed. The total change in volume of the cone was 0.068%. Total CPU time consumed was 239.3 seconds.

The second test case was a hypersonic plane configuration. Twelve cross sections with 13 points per cross section were used to model the shape. Of these 156 points, 40 were fixed thus yielding 116 points that were allowed to be perturbed resulting in 232 design variables (2 coordinates per point). The original configuration (Figure 4) had constraints placed so that the vertical tails, wings and engine housing would remain constant in shape. The arrows again indicate the fixed points. Figure 5 shows a three dimensional view of the original configuration. After 51 optimization cycles, a drag reduction of 64.5% was achieved. Figures 6, 7 and 8 show the final optimized configuration. Note that the inlet to the engine has been smoothed out by the optimization routine, removing the sharp inlet shape. A 0.12% change occurred in the volume. Total CPU time was 251.5 seconds confirming that this code could be run on a personal computer with 20 Mb of RAM.

Convergence histories showing the percent of original drag remaining for these two runs are plotted in Figure 9. Both runs show a smooth monotonic decrease in drag toward convergence.

## CONCLUSIONS

A cost-effective procedure for preliminary shape design optimization of arbitrarily shaped hypersonic vehicles has been shown to significantly reduce aerodynamic wave drag while keeping the vehicle's volume and length constant. This formulation is fast only because a modified Newtonian flow theory was used as the flow field analysis algorithm. The point motion algorithm can be used to keep parts of the original vehicle, such as engine or cabin size or wing thickness, fixed during the optimization. More sophisticated flow field solvers that include viscosity and the effects of heat transfer could be substituted in place of the modified Newtonian flow theory during a few of the final optimization cycles.

## ACKNOWLEDGEMENTS

Many thanks are due to Mr. Zvi Weinberg for his invaluable assistance in producing the graphics for this paper. The authors would also like to thank Apple Computer, Inc. for their donated equipment.

## REFERENCES

1. Dulikravich, G. S, Buss, R. N., Strang, E. J. and Lee, S., "Aerodynamic Shape Optimization of Hypersonic Missiles", AIAA Paper 90-3073, Proc. of the AIAA 8th Applied Aerodyn. Conf., Portland, OR, August 20-22, 1990.
2. Lee, J. and Mason, W. H., "Development of an Efficient Inverse Method for Supersonic and Hypersonic Body Design", AIAA Paper 91-0395, 29th Aerospace Sciences Meeting, Reno, Nevada, January 7-10, 1991.
3. Blankson, I., "Hypersonic Waveriders: State of the Concept", AIAA Paper 91-0529, AIAA Aerospace Sciences Meet., Reno, NV, Jan. 7-10, 1991.
4. Dulikravich, G.S. and Sheffer, S.G., "Aerodynamic Shape Optimization of Arbitrary Hypersonic Vehicles", Proc. of 3rd Internat. Conf. on Inverse Design Concepts and Optimizat. in Eng. Sci. (ICIDES-III), Edt: G.S. Dulikravich, Washington, D.C., Oct. 23-25, 1991.
5. Anderson, J. D. Jr., Hypersonic and High Temperature Gas Dynamics, McGraw-Hill, New York, 1989.
6. Cox, R.N. and Crabtree, L.F., Elements of Hypersonic Aerodynamics, Academic Press, New York, 1965.
7. Geiger, R. E., "Experimental Lift and Drag of a Series of Glide Configurations at Mach Numbers 12.6 and 17.5," *Journal of Aerospace Sciences*, April 1962, pp. 410-419.
8. Prof. Ashok Belegundu, private communications, Department of Mechanical Engineering, Penn State University, Spring 1989.
9. Pshenichny, B. N and Danilin, Y. M., Numerical Methods in Extremal Problems, MIR Publishers, Moscow, 1969.
10. Dulikravich, G.S. and Sheffer, S.G., "Aerodynamic Shape Optimization of Hypersonic Configurations Including Viscous Effects", AIAA 92-2635, AIAA 10th Applied Aerodynamics Conference, Palo Alto, CA, June 22-24, 1992.

Test Case	Drag reduction (%)	No. of optimiz. cycles	No. of analysis calls	CPU on IBM 3090 (sec)
Cone	25.2%	39	7,753	239.3
Hyperson Plane	64.5%	51	11,801	251.5

Table 1. Drag reduction, number of optimization cycles, number of analysis calls and CPU time for the two test cases using the point motion algorithm and individual constrained points.

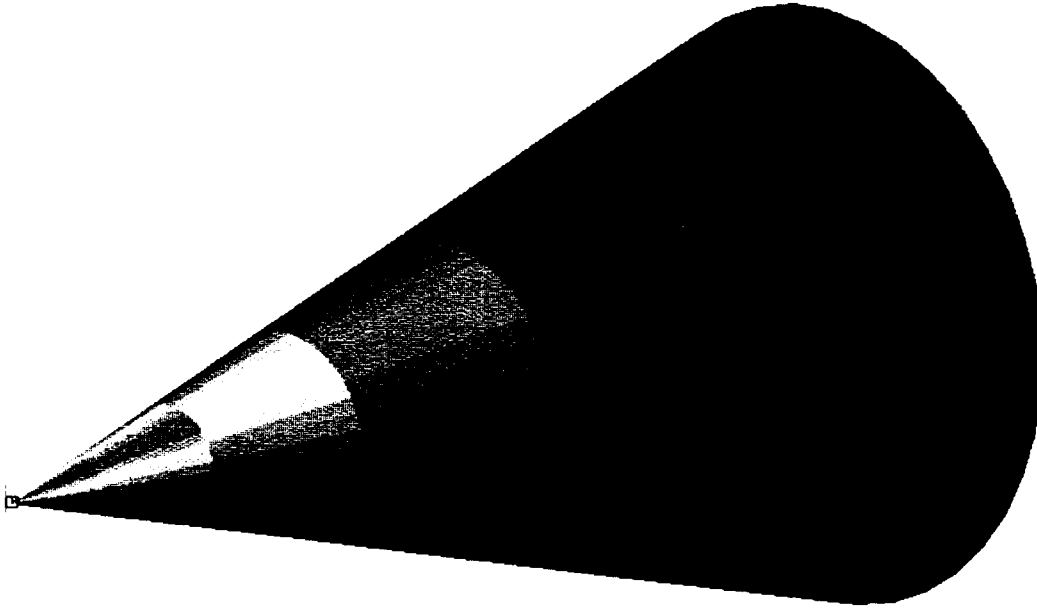


Figure 1. Original configuration of the right circular cone.

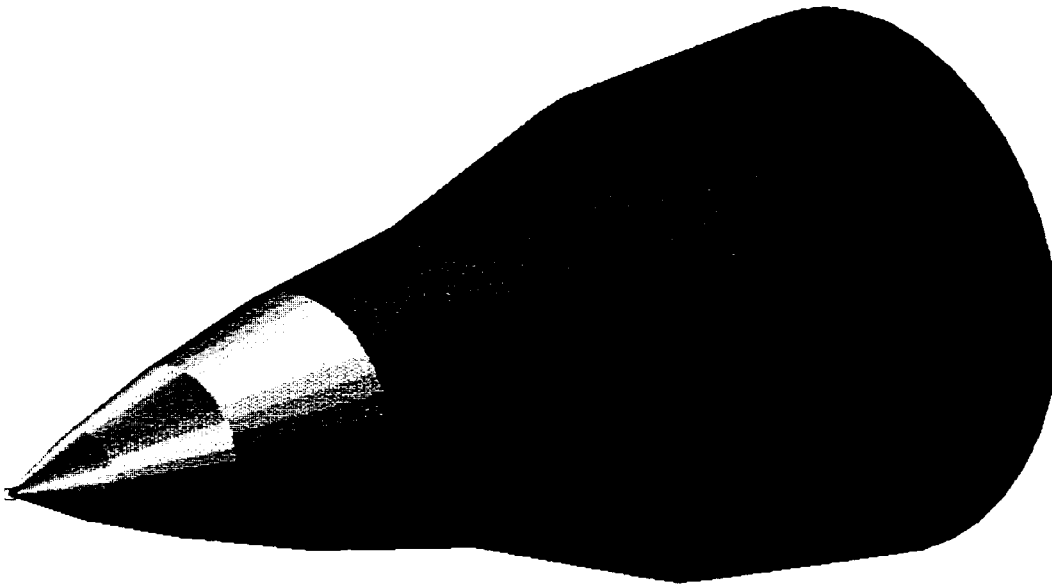


Figure 2. Final optimized shape for the right circular cone.

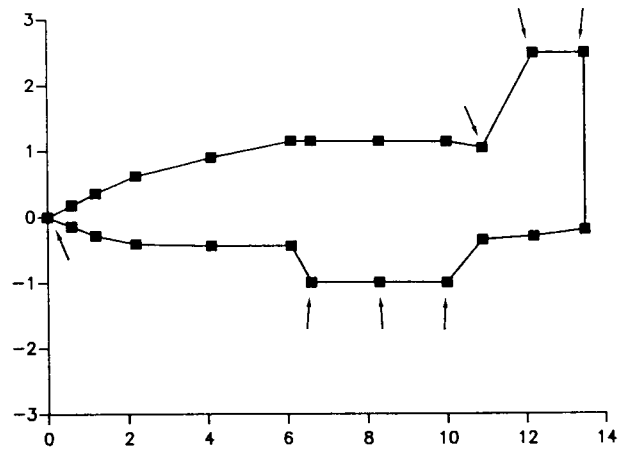
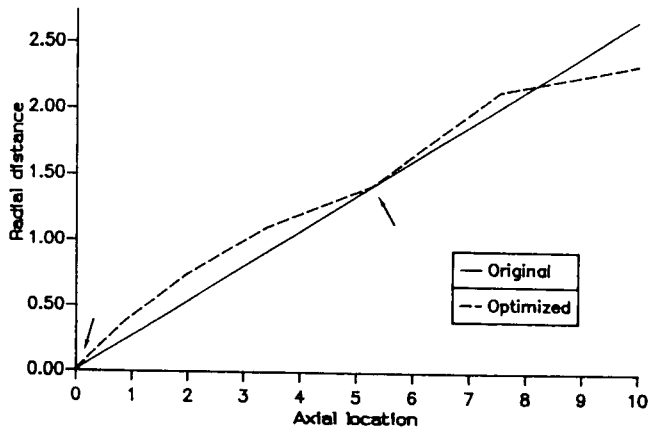


Figure 3. Radius variation of the original and optimized right circular cone. Arrows indicate constrained cross sections.

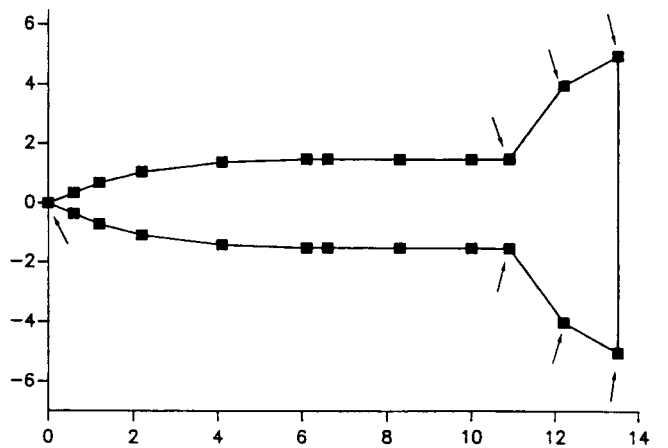
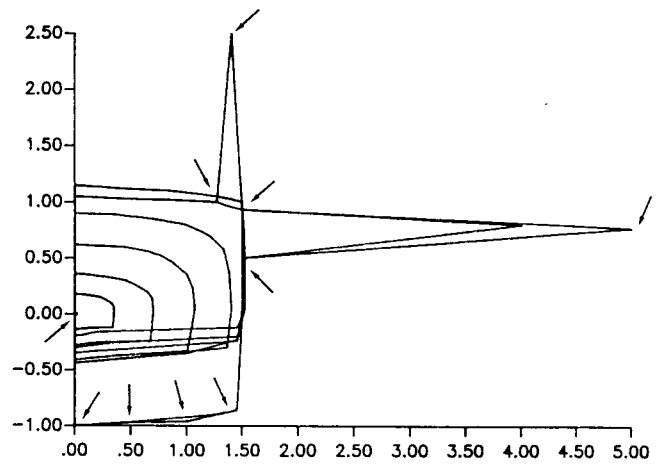


Figure 4. Original configuration for the hypersonic plane. Arrows indicate constrained points.



Figure 5. Original configuration (with pressure distribution) for the hypersonic plane.



Figure 6. Final optimized configuration for the hypersonic plane.



Figure 7. Final optimized configuration for the hypersonic plane, side view.

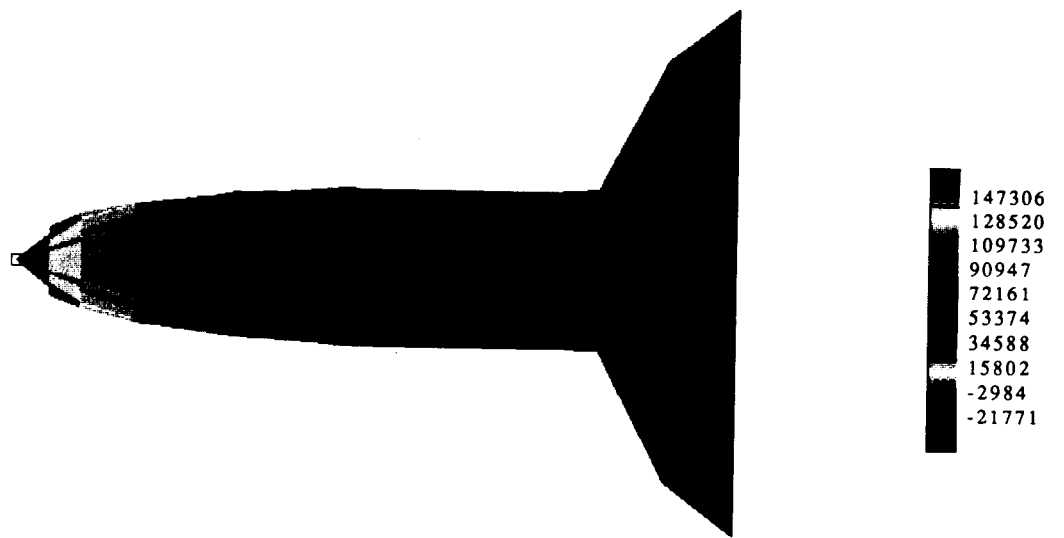


Figure 8. Final optimized configuration for the hypersonic plane, top view.

Percent of original drag remaining vs. iteration

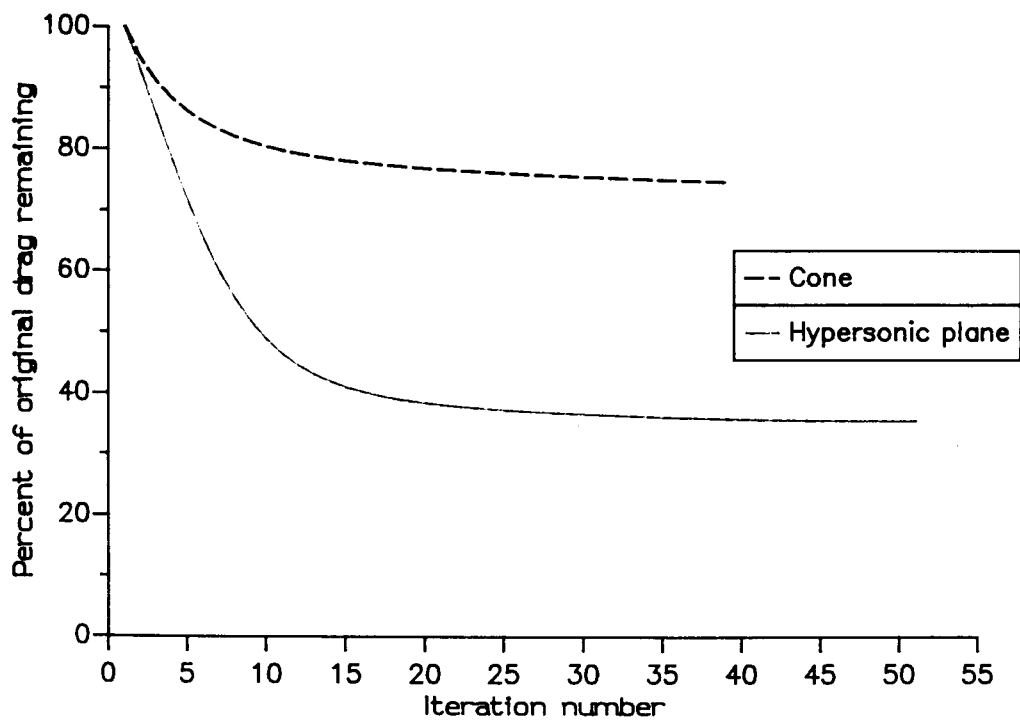


Figure 9. Convergence histories for the cone and hypersonic plane using the point-motion algorithm and individually constrained points; normalized drag reduction.